Desalination and Water Treatment
www.deswater.com
doi: 10.1080/19443994.2013.830687

52 (2014) 7460–7467
December

Taylor & Francis
Taylor & Francis Group

The effects of GAC adsorption on DOM structure and size distribution changes with time

Seon-Ha Chae[a], Seong-Su Kim[a], Ji-Young Moon[b], Woochang Jeong[c], No-Suk Park[d,*]

[a]*Water Research Center, Korea Institute of Water and Environment, Korea Water Resources Corporation, 462-1, Jeonmin-Dong, Yusung-Gu, Daejeon 305730, Korea*
[b]*Water Supply Analysis and Improvement Team, Water Supply and Maintenance Deptartment, Korea Water Resources Corporation, 200 Sintanjin-Ro, Daedeok-Gu, Daejeon 306711, Korea*
[c]*Department of Civil Engineering, Kyungnam University, Changwon, Korea*
[d]*Department of Civil Engineering, Gyeongsang National University, 501, Jinju-daero, Jinju 660-701, Korea*
Tel. +82 55 772 1798; Fax: +82 55 772 1799; email: nspark@gnu.ac.kr

Received 19 July 2012; Accepted 18 July 2013

ABSTRACT

The primary objectives of this study were to investigate the effects of granular activated carbon (GAC) adsorption on dissolved organic matter (DOM) and changes in structure and size distribution with time to establish the interrelationships between its breakthrough and size distribution through pilot-scale and rapid small-scale column testing (RSSCT). Results indicate that most hydrophobic DOM (HPO) was removed at the beginning of testing, and the removal efficiency decreased with time. In addition, hydrophilic DOM concentration was unchanged. Therefore, it was determined that HPO and transphilic DOM (THP) was affected by GAC adsorption. Moreover, organic matter of the 1–3 K size range was affected the most by GAC adsorption. As GAC breakthrough progressed, number average molecular weight (Mn) increased slowly. The ρ index, which represents the weight average molecular weight: Mn ratio and is used to determine polydispersivity, peaked at the beginning of RSSCT. As bed volumes increased with the progress of adsorption, ρ decreased.

Keywords: Granular activated carbon (GAC); GAC adsorption; Molecular weight; Dissolved organic matter; Size distribution

1. Introduction

The granular activated carbon (GAC) adsorption process is widely used to remove synthetic organic compounds (SOCs) and natural dissolved organic matter (DOM) from water. However, when these two elements coexist, it has been reported that DOM could interfere with removal of the targeted SOCs by GAC adsorption [1–3]. This is because the relatively high concentration of DOM creates strong competition with various target pollutants in securing pore space of GAC. GAC adsorption capacity for the removal of DOM depends on the pore size and surface acidity of GAC and the size distribution and chemical ingredients of DOM. Given that GAC particle surfaces are generally nonpolarized and hydrophobic (HPO), organic matter with a molecular weight of less than 40 K can be easily adsorbed onto GAC. On the contrary, hydrophilic (HPI) and organic matter of high

*Corresponding author.

molecular weight such as humin does not diffuse easily into GAC micropores; thus, adsorption is difficult [4].

Previous research on chemical ingredients and DOM structure has focused on DOM behavior and its structural adsorption characteristics during the GAC adsorption process. At the beginning of GAC adsorption, humic matter fractions can be selectively removed, allowing only nonhumic matter to be dissolved. Nonhumic organic matter includes those of high-molecular weights such as polysaccharides and HPI matter that tends to remain in water. Karanfil reported that even though the molecular weights of fulvic acids are lower than those of humic acids, the adsorption capacity of the former is lower due to the their HPI characteristics and higher solubility in water [5]. In addition, Semmens and Staples suggested that effluent from the GAC adsorption process contains HPI neutral and acidic organic matter [6].

The size-exclusion GAC-adsorption mechanism considers DOM size. The average size of DOM molecules is generally 4–60 Å [7]. It has been reported that removal efficiency of such DOM can be maximized by a GAC mesopore size of 20–100 Å [8,9]. Previous research has documented size-exclusion effects [10,11]. In addition, Summers and Roberts reported the selectively competitive adsorption of humic acid solutions [12]. However, the effects of GAC adsorption on DOM size distribution have not been investigated thoroughly. Generally, as the molecular weight of DOM increases, its HPO property increases, diffusivity and solubility decrease, and adsorption capacity ultimately increases. The adsorption capacity of relatively large-sized DOM can be affected significantly by GAC size, whereas that of small-sized DOM is not [13].

In this study, the effects of GAC adsorption on DOM structure and size distribution change with time were examined, and the interrelationships between its breakthrough and size distribution were investigated.

2. Materials and methods

2.1. Source water

The water used to test the effects of GAC adsorption on DOM structural change was sourced from Paldang Dam in Korea. According to a pilot-scale test on this water, the average values of dissolved organic carbon (DOC) and UV254 absorbance were 1.6 mg/L and 3.67 m^{-1}, respectively. In addition, other sand-filtered water samples used for a rapid small-scale column test (RSSCT) to investigate molecular weight and size distribution changes of DOM. The DOC and UV254 average values of these samples were 1.7 mg/L and 6.4 m^{-1}, respectively.

2.2. Analysis methods

Distribution of HPO DOM, THP DOM, and HPI DOM was measured on the condition of less than pH 2 by the resin columns composed of XAD-8 and XAD-4 (SUPELCO, USA). HPO could be absorbed onto XAD-8 only, and THP was absorbed onto XAD-4 only. The unabsorbed HPI remained within the effluent from the resin column. DOM separation using these resin columns proceeded as follows: column filling, column cleansing, sample preparation, sample operation, and extraction (refer to Fig. 1).

Glass columns (Spectrum Chromatography Ltd.) with inner diameters of 1 cm were filled with 10 mL XAD-8 and 40 mL XAD-4, and repeatedly cleaned with ultrapure water in addition to acidic (0.1 N, H_3PO_4) and basic solutions (0.1 N, NaOH). To examine degrees of clarity, a 0.1 N solution of NaOH was filtered through the columns, and DOC concentrations from the injected and the filtered solutions were measured. The column-cleansing process was considered satisfactory if the difference between both concentrations was less than 0.1 mg/L. H_3PO_4 was added to a 600 mL water sample to adjust its pH to less than 2 ± 0.1, and the sample was filtered through 0.45-μm filter paper. The pH was adjusted to keep the sample acidic neutralized and relatively HPO for measuring DOC concentration and UV254 absorbance.

The prepared sample was then passed through the XAD-8 and XAD-4 resin columns at 2.0 mL/min, and the final effluent from both columns was gathered into a dark brown glass bottle. The DOM absorbed on the columns was extracted with a 0.1 N NaOH solution at a relatively low flow rate of 1.0 mL/min. The DOM extracted from XAD-8 and XAD-4 were HPO and THP, respectively. The DOC concentration and UV254

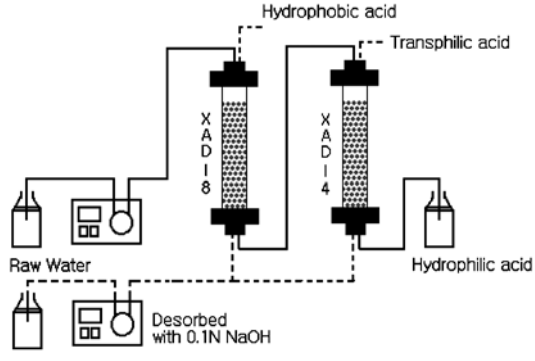

Fig. 1. DOM separation system.

absorbance of each respective effluent were measured to determine the recovery rate during separation. The ideal recovery rate range is approximately 90 ± 0.5%.

For DOC concentration analysis, we adopted standard method 5310C, the Persulfate-Ultraviolet Oxidation Method [14]. We examined the total organic carbon with a standard analyzer (Phoenix 8000, Dohrman). In addition, a spectrophotometer (Cary 5G UV-vis-NIR, Varian) and 1-cm quartz cells were used for detecting UV254 absorbance. The values were represented as total absorbance divided by the cell length in dimensions of m^{-1}. To evaluate DOM size distribution, the high-performance size-exclusion chromatograph (HPSEC) method was used with high-performance liquid chromatography and size-exclusion chromatography columns. The UV analyzer used as a detector for HPLC consisted of a high-pressure pump (Perkin–Elmer LC 200), diode array UV detector (Perkin–Elmer 235C), and filtration column (Waters Protein-Pak 125). A 4 mM phosphate buffer solution was used for elution, and NaCl was used to strengthen ion intensity to approximately 0.1 M. The flow rate for column filtration was set to 1.0 mL/min.

Polystyrene sulfornates (PSS) with molecular weights of 1.8, 4.6, 8, and 18 K were used as standard reference materials to characterize humic substances.

We determined the first-order standard curve from PSS using the HPSEC method, and the target DOM was calculated using weight average molecular weight (Mw), number average molecular weight (Mn), and polydispersivity (ρ; the ratio of Mw and Mn) (Fig. 2). The standard curve derived from this study is given as Eq. (1).

$$\log(\mathrm{Mw}) = -0.5212t + 7.9038,\ R^2 = 0.997 \tag{1}$$

where t is retention time at peak.

Mn and Mw of each sample were determined by the following equations [15]:

$$\mathrm{Mn} = \frac{\sum_{i=1}^{n} h_i}{\sum_{i=1}^{n} \frac{h_i}{M_i}} \tag{2}$$

$$\mathrm{Mw} = \frac{\sum_{i=1}^{n} h_i M_i}{\sum_{i=1}^{n} h_i} \tag{3}$$

where h_i is the height (detector response after baseline correction) of the sample HPSEC curve eluted at volume i or at retention time R_t; and M_i is the molecular weight at eluted volume i or at retention time R_t, determined from the standard calibration curve.

2.3. Experimental methods

To investigate the effects of GAC adsorption on DOM structural change with time, we conducted pilot tests. Pilot-scale GAC adsorbers consisted of two gravitational fixed bed-type columns. The inlet flow rate was 8.3 m^3/d and the linear velocity was 5.6 m/h. The two columns were filled with activated carbon (AC; Calgon, Ltd.) according to empty bed contact times (EBCTs) of 7 and 14 min. RSSCT was used to simulate the performance of large-scale GAC columns. The proportional diffusivity was employed for RSSCT design and its equations used are shown in Eqs. (4)–(6).

$$\frac{\mathrm{EBCT_{SC}}}{\mathrm{EBCT_{LC}}} = \frac{d_{\mathrm{SC}}}{d_{\mathrm{LC}}} = \frac{t_{\mathrm{SC}}}{t_{\mathrm{LC}}} \tag{4}$$

$$\frac{v_{\mathrm{SC}}}{v_{\mathrm{LC}}} = \frac{d_{\mathrm{LC}}}{d_{\mathrm{SC}}} \frac{\mathrm{Re}_{SC,\min}}{\mathrm{Re}_{\mathrm{LC}}} \tag{5}$$

$$Re_{LC} = \frac{\rho d_{\mathrm{LC}} v_{\mathrm{LC}}}{\mu} \tag{6}$$

where EBCT are the EBCTs, d is the absorbent particle diameter, t is the elapsed times, v is the velocity (i.e. hydraulic loading rate), $\mathrm{Re}_{SC,\min}$ is the minimum Reynolds number of small column, $\mathrm{Re_{LC}}$ is the Reynolds number of the field scale column, ρ is the density, and μ is the water viscosity; SC and LS in subscript represent the small and larger scale column, respectively.

To evaluate the effects of GAC adsorption on DOM-size distribution change with time, we conducted

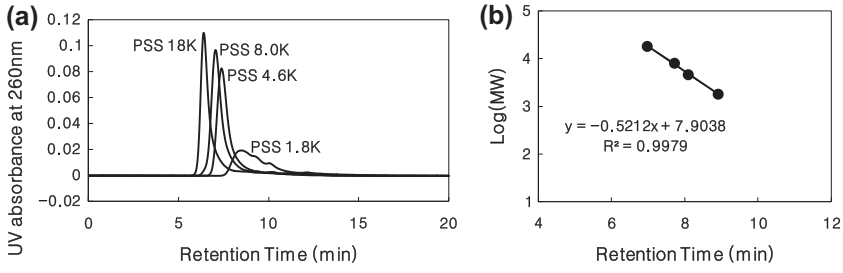

Fig. 2. (a) HPSEC data and (b) standard curve from PSS.

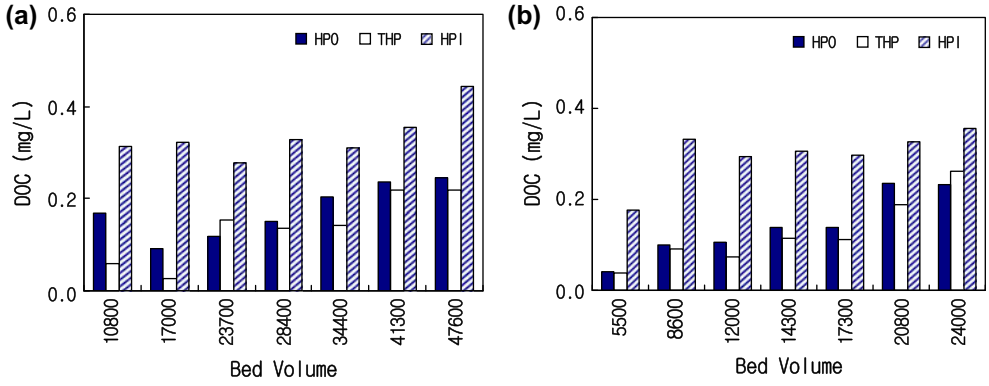

Fig. 3. DOC concentrations of HPO dissolved organic material (DOM; HPO), THP DOM, and HPI DOM according to bed volumes at EBCTs of (a) 7 min and (b) 14 min.

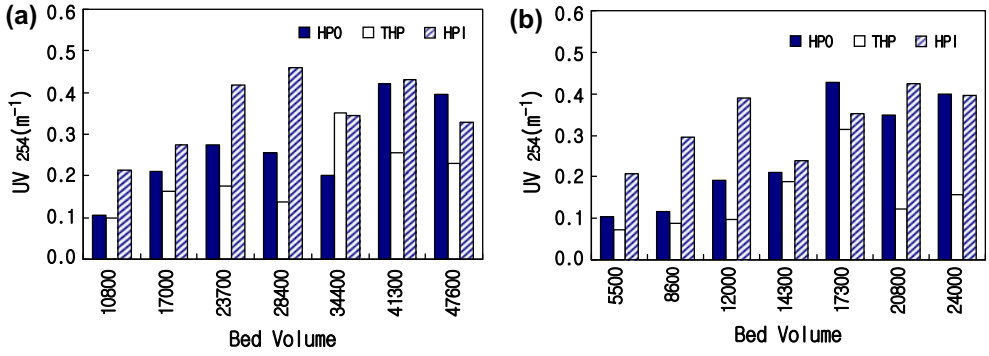

Fig. 4. UV254 absorbance of HPO dissolved organic material (DOM; HPO), THP DOM, and HPI DOM according to bed volumes at EBCTs of (a) 7 min and (b) 14 min.

Table 1
Distribution ratios of each type of dissolved organic matter (DOM) after separation

Bed volumes	Condition	Dissolved organic carbon (%)			UV254 absorbance (%)		
		HPO	THP	HPI	HPO	THP	HPI
10,800	Empty bed contact time (EBCT): 7 min	16.9	11.2	71.9	25.2	23.8	51.1
17,000		21.1	6.1	72.9	32.6	25.0	42.4
23,700		21.6	27.9	50.5	31.8	20.1	48.1
28,400		24.4	22.2	53.4	30.0	16.1	54.0
34,400		31.1	21.6	47.7	22.4	39.0	38.5
41,300		29.2	27.0	43.8	38.0	23.0	38.9
47,600		27.0	24.0	49.0	41.6	23.9	34.5
5,500	Empty bed contact time (EBCT): 14 min	16.3	15.0	68.7	26.9	19.2	54.0
8,600		19.2	17.5	63.3	23.5	17.8	58.7
12,000		22.2	15.8	62.1	28.3	14.3	57.4
14,300		24.8	20.5	54.6	33.1	29.4	37.5
17,300		25.0	20.5	54.5	39.1	28.8	32.2
20,800		31.3	25.2	43.5	38.9	13.7	47.4
24,000		27.4	30.8	41.8	42.0	16.5	41.5

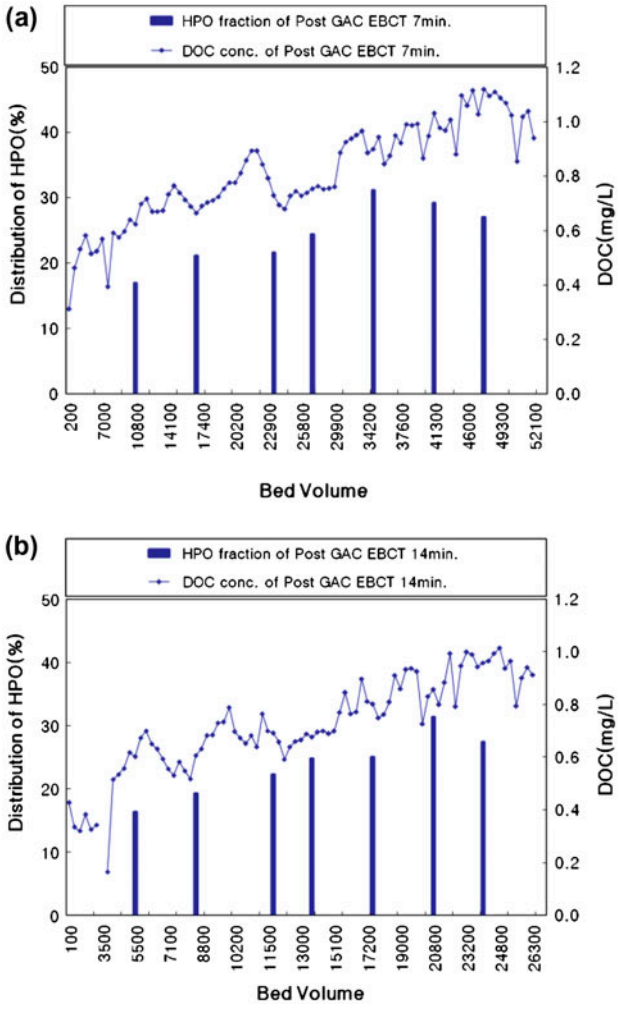

Fig. 5. DOC concentration and ratio of HPO dissolved organic material (HPO) according to bed volumes at EBCTs of (a) 7 min and (b) 14 min.

RSSCT according to the information collection request manual of the Environmental Protection Agency [16–18]. This test used 100 × 200 mesh GAC with a continuous flow rate of 2.0 mL/min ± 2% and EBCT of 1.06 min for simulating the 10-min full-scale EBCT. The inner diameter of the small-scale column was 4.76 mm, and the depth of GAC bed was 12 cm.

3. Results and discussion

3.1. Effects of GAC adsorption on DOM structural change

In the case of the source water obtained from Paldang Dam, average fractions of HPI, HPO, and THP were 43.9, 37.6, and 18.7%, respectively. The HPO–HPI component ratio became more analogous with time. In the case of the sand-filtered water, the average percentages of HPI, HPO, and THP were 50.0, 32.2, and 17.8%, respectively. The HPI percentage of the sand-filtered water was relatively higher because THP and HPI were not removed as effectively through conventional treatment processes, which generally consist of flocculation, sedimentation, and filtration. Of the total DOC, only HPO was removed.

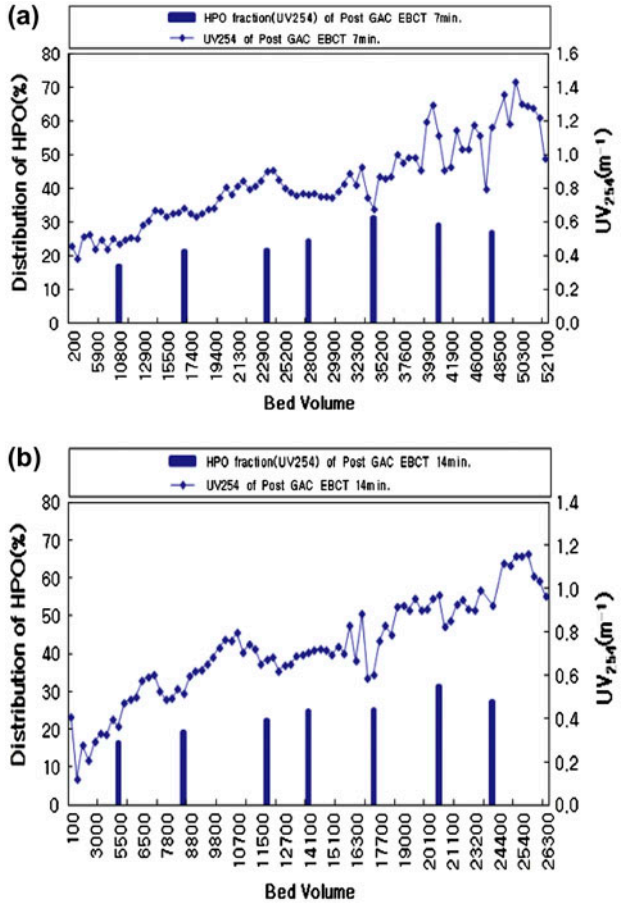

Fig. 6. UV254 absorbance and that of HPO dissolved organic material (HPO) according to bed volumes at EBCTs of (a) 7 min and (b) 14 min.

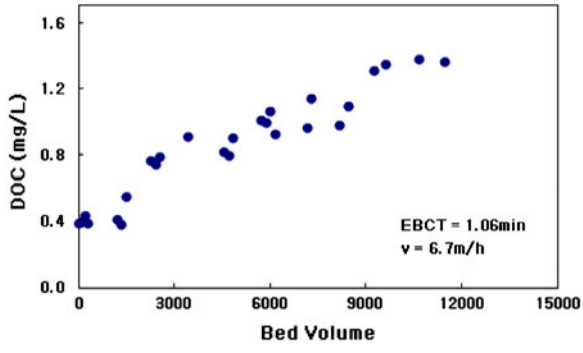

Fig. 7. DOC breakthrough curve according to bed volumes.

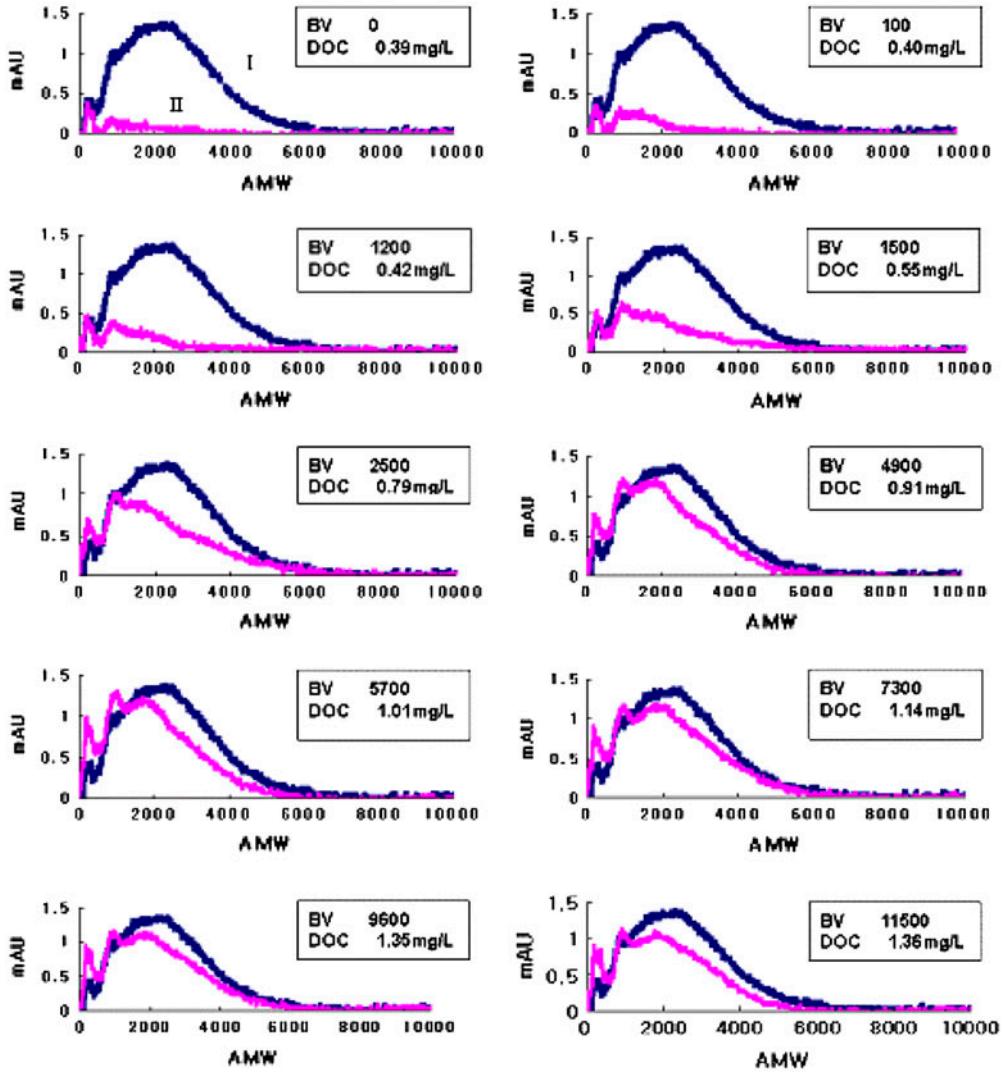

Fig. 8. Molecular size distribution of organic matter according to bed volumes. The dark navy color represents influent and effluent is plotted in magenta.

Figs. 3 and 4 show HPO, THP, and HPI concentrations in addition to UV254 absorbance according to bed volumes, and Table 1 summarizes the distribution ratio of each DOM after separation. Bed volume is a type of indicator that represents cumulative throughput during adsorption by GAC unit volume and is dimensionless. As bed volumes increased, the HPO ratio increased steeply and THP increased gradually. On the contrary, the HPI ratio was nearly unchanged. The results of UV254 absorbance measurement were similar to the distribution ratio of the three types of DOM. In the case of EBCT, at 7 min, the distribution ratios of each DOM were 71.9% (HPI), 16.9% (HPO), and 11.2% (THP) in the early stages of adsorption. The ratios of EBCT at 14 min were similar to that at EBCT 7 min. This may have occurred because in the early stages of adsorption, HS and HPO could be selectively removed, whereas nonhumic substances of high molecular weight and HPI organic matter remained. Accordingly, the GAC adsorption capacity of HPO is greater than that of HPI and THP. As adsorption progressed, the adsorption capacity of HPO decreased, and so did the total DOC removal efficiency. That is, HPO removal efficiency decreased much more than that of HPI and THP. THP and HPO were affected by GAC adsorption because the THP ratio increased with adsorption time.

Fig. 5 shows DOC concentration and HPO ratio according to bed volumes, and Fig. 6 shows UV254 absorbance and that of HPO according to bed vol-

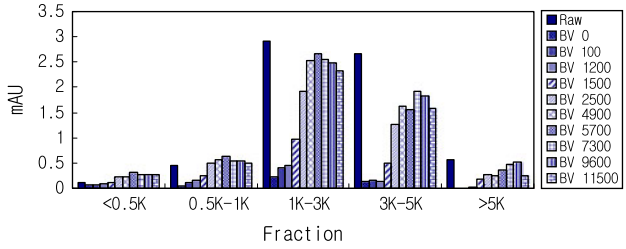

Fig. 9. Change in AMW component ratios under various bed volume conditions.

umes. As adsorption processed, the HPO ratio, DOC concentration, and UV254 absorbance clearly increased. As noted previously, the removal efficiency of HPO was relatively high in the early stages of adsorption and decreased steeply over time.

3.2. Effects of GAC adsorption on DOM size distribution change

Fig. 7 shows the DOC breakthrough curve on bed volume as a plot of the RSSCT results for the sand-filtered water, as described in the Experimental Methods section. The nonadsorptive matter ratio of DOC in the influent was approximately 25%. The results of DOM separation revealed HPI, HPO, and THP fractions of 23.4, 61.7, and 14.9%, respectively. The nonadsorptive matter ratio from RSSCT was in good agreement with the HPI ratio from DOM separation [19]. As can be seen in Fig. 7, DOC concentration within effluent from the small-scale column increased gradually and reached a steady state after the initial breakthrough. The concentration continued to increase, ultimately reaching 80% of influent with a bed volume of 11,500.

The results of this study can be used for evaluating water treatment processes. As can be inferred from the HPSEC results (Fig. 8), the apparent molecular weight (AMW) of most of the DOM in the influent was less than 6 K. In addition, Figs. 7 and 8 show that the Mw of nonadsorptive organic matter, which could not be removed from the small-scale column in the early stages, was less than 0.3 K. Mid-sized organic matter of 1–2 K increased sharply when bed volume was 2,500 of which 52% DOC was removed. Finally, the maximum specific deposit within the effluent was similar to that within the influent when bed volume approached 9,600. Such bed volume conditions are in accordance with the condition in which DOC removal ceased (Fig. 7). Thus, the analysis of molecular size distribution could enable prediction of the characteristics of DOC breakthrough within GAC absorbers.

Fig. 9 shows changes in AMW component ratios of effluent from the GAC column. Organic matter was categorized into five AMW ranges: <0.5, 0.5–1, 1–3, 3–5, and >5 K. The dominant influent range was 1–5 k. When bed volume reached 2,500, the portion of organic matter of the range <0.5 K was higher in the effluent than in the influent. In addition, the proportion of organic matter of the 1–3 K range was close to 80% of the influent after the bed volume reached 7,300. As bed volumes increased, the ratio of organic matter of the 1–5 K range increased. These results indicate that organic matter of 1–3 K size range is the most affected by GAC adsorption.

Table 2 summarizes the Mn and Mw from the results of HPSEC. As GAC breakthrough progressed, MN increased slowly. Although Mw values were larger than those of Mn, the rate change was slight, and no trend was detected. Moreover, an interrelationship with the DOC breakthrough curve was not apparent. The ρ index, which represents the Mw:Mn ratio and is used to determine polydispersivity, was highest at the beginning of RSSCT. As the bed volumes increased through the adsorption process, ρ decreased. These results were attributed to the molecular size distribution being concentrated in the <0.5 K size range at the beginning of RSSCT, which then shifted to the 1–3 K size range as the GAC adsorption progressed.

Table 2
Mn, Mw, and polydispersivity (ρ; the ratio of Mw and Mn) of influent and effluent

Division	Influent	Bed volumes									
		0	100	1,200	1,500	2,500	1900	5,700	7,300	9,600	11,500
Mn	2,540	1,412	1,662	1826	1941	1960	1971	2,208	2,245	2,338	2030
Mw	3,353	3,333	3,046	3,324	2,705	2,679	2,384	3,421	3,116	3,488	2,734
ρ (Mw/Mn)	1.32	2.36	1.83	1.82	1.39	1.37	1.20	1.55	1.39	1.49	1.35

4. Conclusions

In this study, we examined the effects of GAC adsorption on DOM structure and size distribution change with time, and investigated the interrelationships between breakthrough and size distribution. Following is a summary of the results of this study:

(1) During the examination of DOC concentration and DOM structure with the progress of GAC adsorption, HPO was mainly removed at the beginning, and its removal efficiency decreased with time. In addition, HPI concentration was unchanged. Thus, HPO and THP were affected by GAC adsorption.
(2) The results of HPSEC and RSCCT indicate that organic matter of the 1–3 K size range is most easily affected by GAC adsorption. In addition, molecular size distribution can be used as a GAC performance indicator to predict the characteristics of DOC breakthrough within the GAC absorber.
(3) As GAC breakthrough progressed, Mn increased gradually. The ρ index was highest at the beginning of RSSCT. As bed volumes increased through the process of adsorption, the ρ index decreased. These results confirmed that the molecular size distribution was in the <0.5 K range at the beginning of RSSCT and shifted to 1–3 K size range as the GAC adsorption progressed.

Acknowledgement

This research was supported by a grant (CTIC-01) from Construction Technology Innovation Program funded by Ministry of Land, Transport and Maritime Affairs of Korean government.

References

[1] H. Sonthmeir, J.C. Crittenden, R.S. Summers, Activated Carbon for Water Treatment, 2nd ed, DVGW-Forschungsstelle, Karlsruhe, 1988.
[2] D.R.U. Knappe, V.L. Snoeyink, P. Roche, M.J. Prados, M.M. Bourbigot, The effect of preloading on rapid small-scale column test predictions of atrazine removal by GAC adsorbers, Water Res. 31 (1997) 2899–2909.
[3] C.J. Corwin, R.S. Summers, Scaling trace organic contaminant adsorption capacity by granular activated carbon, Environ. Sci. Technol. 44(14) (2010) 5403–5408.
[4] M. Kitis, Probing chlorine reactivity of dissolved organic matter for disinfection by-products (DBP) Formation: Relations with specific ultraviolet absorbance (SUVA) and development of the DBP reactivity profile, PhD Dissertation, Clemson University, Clemson, SC, 2001.
[5] T. Karanfil, M. Kitis, J.E. Kilduff, M.A. Schlautman, W.J. Weber, Adsorption of organic macromolecules by granular activated carbon: 1. Influence of molecular properties under anoxic solution conditions, Environ. Sci. Technol. 30 (1996) 2187–2194.
[6] M.J. Semmens, A.B. Staples, The nature of organics removed during treatment of Mississippi River water, J. AWWA 78 (1986) 76–81.
[7] E.M. Thurman, R.I. Malcomn, Preparative isolation of aquatic humic substance, Environ. Sci. Technol. 15 (1981) 463–466.
[8] T. Karanfil, M. Kitis, J.E. Kilduff, A. Wigton, Role of granular activated carbon surface chemistry on the adsorption of organic compounds, 2. Natural organic matter, Environ. Sci. Technol. 33 (1999) 3225–3233.
[9] T. Karanfil, J.E. Kilduff, Role of granular activated carbon surface chemistry on the adsorption of organic compounds, 1. Priority pollutants, Environ. Sci. Technol. 33 (1999) 3217–3224.
[10] J.E. Kilduff, A. Wigton, Sorption of TCE by humic-preloaded activated carbon: Incorporating size-exclusion and pore blockage phenomena in a competitive adsorption model, Environ. Sci. Technol. 33 (1996) 250–256.
[11] W.J. Weber, Jr., T. C. Voice, A. Jodelah, Adsorption of humic substances: The effects of heterogeneity and system characteristics, J. AWWA 75 (1983) 612–619.
[12] R.S. Summers, P.V. Roberts, J. Colloid Interface Sci., Activated carbon adsorption of humic substance, I. Heterodisperse mixtures and desorption 122 (1988) 367–381.
[13] E.K. James, Water Quality & Treatment: A Handbook on Drinking Water, 6th ed., American Water Works Association, New York, 2011.
[14] APHA, AWWA, WEF, Standard Methods for the Examination of Water and Wastewater, 21st ed., Washington, DC, 2005.
[15] Q. Zhou, S.E. Cabaniss, P.A. Maurice, Considerations in the use of high-pressure size exclusion chromatography (HPSEC) for determining molecular weights of aquatic humic substances, Water Res. 34 (2000) 3505–3514.
[16] R.S. Summers, S. Hopper, S. Hong, GAC Precursor Removal Studies, ICR Manual for Bench-and Pilot-scale Treatment, EPA 814-B-96-003, USEPA, Officer of Water, 1996.
[17] J.C. Crittenden, P.S. Reddy, H. Arora, J. Trynoski, D.W. Hand, D.L. Perram, R.S. Summers, Predicting GAC performance with rapid small-scale column tests, J. AWWA 83(1) (1991) 77–87.
[18] T.E.T. Gillogly, V.L. Snoeyink, J.C. Vogel, C.M. Wilson, E.P. Royal, Determining GAC bed life, J. AWWA 91(8) (1999) 98–110.
[19] R.S. Summers, D.R.U. Knappe, V.L. Snoeyink, Adsorption of organic compounds by activated carbon, in: J. Edzwald (Ed.), Water Quality and Treatment, McGraw-Hill, New York, NY, 2010.